Entropy Generation Analysis of Natural Convection in a Porous Medium with Casson Fluid using Finite Element Method

Bai Cham , Shams Ul Islam , Suvash C Saha *

Posted Date: 28 July 2023

doi: 10.20944/preprints202307.1968.v1

Keywords: Casson Fluid; Entropy generation; Heat Transfer; Porous medium; Finite Element Method; Natural Convection.

Article

Entropy Generation Analysis of Natural Convection in a Porous Medium with Casson Fluid Using Finite Element Method

Bai Mbye Cham [1,3], Shams-ul-Islam [2] and Suvash C. Saha [2,*]

[1] Department of Mathematics, COMSATS University Islamabad, Islamabad Campus, Park Road, Tarlai Kalan, Islamabad 45550, Pakistan; bmcham@utg.edu.gm, islam_shams@comsats.edu.pk
[2] School of Mechanical and Mechatronic Engineering, University of Technology Sydney (UTS), NSW 2007, Australia; Suvash.Saha@uts.edu.au
[3] Department of Mathematics, University of The Gambia, P.O. Box 3530, Serrekunda, The Gambia.
* Correspondence: Suvash.Saha@uts.edu.au; Tel.: +61-295143183;

Abstract: This study presents a comprehensive investigation of entropy generation during natural convection in a porous medium with Casson fluid. The governing equations, including the momentum, energy, and entropy balance equations, are solved numerically using finite element method. Through the analysis, various parameters affecting entropy generation are investigated, such as the Casson fluid parameter, Radiation, Prandtl number, and Rayleigh number. The results indicate that the Casson fluid parameter significantly influences the flow and heat transfer characteristics, while the Darcy number and Rayleigh number control the intensity of natural convection. Moreover, the Prandtl number determines the relative significance of heat transfer compared to viscous effects.

Keywords: casson fluid; entropy generation; heat transfer; porous medium; finite element method; natural convection

1. Introduction

Natural convection in a porous medium with non-Newtonian Casson fluid has gained significant attention due to its application in various industrial and environmental processes. The study of entropy generation in such systems plays a crucial role in understanding the irreversibilities and inefficiencies inherent in the heat transfer process [1,2]. In this context, the Finite Element Method (FEM) emerges as a powerful numerical tool for conducting detailed analyses. This study performs the entropy generation analysis of natural convection in a porous medium with Casson fluid and highlights the importance of employing FEM as a computational technique for studying the intricate interplay of fluid dynamics and heat transfer in complex systems. By investigating entropy generation, researchers gain valuable insights into optimizing energy transfer and enhancing the overall efficiency of natural convection processes with profound implications for a wide range of engineering and environmental applications.

Casson fluid are shear thinning fluid which return to their original form when applied shear stress is release. These type of fluids are been categorize as viscoelastic. The rheological model has been successfully applied to various fields, including food processing, pharmaceuticals, cosmetics, and oil drilling, so as to understand and predict the flow behavior of non-Newtonian materials. However, its utilization in the context of natural convection and entropy generation within the Darcy-Forchheimer model remains relatively unexplored. Pop et al. [3] in a pioneering study, investigated the heat transfer systems of Casson fluid inside a square enclosure subjected to temperature differences. The results provided insights into the convective heat transfer characteristics and can be utilized to optimize systems involving Casson fluids subjected to thermal radiation and viscous dissipation effects. Hamid et al. [4] investigated the fluid flow phenomena inside a trapezoidal enclosure containing a Casson fluid. Furthermore, Aneja et al. [5] examined Casson fluid in a buoyancy induced convective phenomena inside a porous hollow that is partially heated. The findings have implications for various engineering

 doi:10.20944/preprints202307.1968.v1

applications and non-Newtonian fluids such as energy systems, environmental engineering, and materials processing. Aghighi et al. [6] investigated double-diffusive natural convection, which involves the simultaneous transport of heat and mass within a fluid due to density differences. The findings of the study revealed the impact of double diffusion and Casson fluid behavior on the flow and temperature distributions within the enclosure. Shah et al. [7] analysed the behavior of Casson fluids in a curved corrugated cavity and the influence of convective heat and mass transport.

Entropy generation can be found in all heat transfer process due to its irreversibility natural process as stated on the second law of thermodynamics. It is the qualitative representation of lost of energy in most systems. Entropy quantifies the rate at which the useful energy in a system degrades into less useful forms, such as thermal energy dissipation. By analyzing entropy generation, valuable insights can be gained regarding the performance and efficiency of convective heat transfer systems. Additionally, the study of entropy generation in natural convection provides valuable insights into the irreversibility's and energy losses associated with convective heat transfer processes. Gireesha et al. [8] focused on the analysis of entropy generation and heat transmission in the flow of Casson fluids within an inclined porous microchannel, considering the effects of viscous and Joule heating. Kotha et al. [9] investigated the behavior of a Casson fluid on a convectively heated surface and analyze the entropy generation characteristics. They consider the influence of viscous dissipation, which arises due to the internal friction of the fluid and leads to the conversion of mechanical energy into heat. Consequently, Sohail et al. [10] examined the behavior of a Casson fluid and analyze the entropy generation characteristics. The behavior of Casson fluids in an enclosure and analysis of convection and thermal radiation characteristics was also studied by Alzahrani et al. [11]. The authors considered the generation of entropy, which quantifies the irreversibility and dissipation of energy within the system. Hossain et al. [12] focused on Casson fluids in a staggered cavity and entropy generation on double diffusive free convection. They consider magnetic effect, which can alter the transfer of heat movements, and the generation of entropy, which represents the irreversible energy loss and dissipation within the system.

In porous media, where fluid flow occurs through a solid matrix with interconnected void spaces, the Brinkman-Forchheimer model is commonly employed to characterise the behaviour of fluid flow. This model accounts for both viscous and inertial effects in porous media flow and has proven to be effective in capturing the flow characteristics in such systems. The Darcy-Forchheimer model provides a valuable framework for analyzing natural convection in porous media, where the convective flow is significantly influenced by the porous structure. It is important to consider that many fluids encountered in practical applications exhibit non-Newtonian behavior, deviating from the classical Newtonian viscosity assumption. Non-Newtonian fluids display complex flow characteristics due to factors such as shear-thinning or shear-thickening behavior, yield stress, and viscoelasticity. Seth et al. [13] investigated the behavior of Casson fluid for a rotating system within a porous enclosure. The presence of the Darcy-Forchheimer porous medium is also considered. Fluid rotation and porosity interaction was observed to affect the flow characteristics. Qawasmeh et al. [14] focused on buoyancy-driven convective heat transmission of the Casson fluid in Darcy-Forchheimer porous media. Furthermore, Farooq et al. [15] considered the non-Darcy model to show the flow of the Casson fluid in an enclosure. Darcy-Forchheimer Casson fluid flow over a stretching sheets was investigated by Zhang et al. [16]. Consequently, Li et al. [17] investigated the effects of activation energy on a Darcy-Forchheimer flow of a Casson fluid through a channel.

The finite element method (FEM) will be employed as a numerical tool to solved the governing equations, accounting for the non-Newtonian behavior of the Casson fluid. This study will contribute to the understanding of the impact of Casson fluid properties, such as yield stress and flow behavior index, on the convective flow patterns, heat transfer characteristics, and entropy generation rates. Finite element analysis (FEA) discretizes the domain into smaller finite elements to approximate the solutions. In the past decades, researchers have explore the use of FEM to analyse fluid flow interaction in complex situation. Among which includes, Raju et al. [18] used FEM to investigate the

Preprints (www.preprints.org) | NOT PEER-REVIEWED | Posted: 28 July 2023 doi:10.20944/preprints202307.1968.v1

free convective flow of the Casson fluid on a vertically inclined plate which indicates that the plate is oriented at an angle relative to the horizontal direction. Reddy et al. [19] studied dissipation effect on fluid flow behavior and can significantly affect the temperature distribution of the fluid. Consequently, Goud et al. [20] considered the flow of the Casson fluid in a vertical plate (oscillating) in a porous enclosure. The plate undergoes oscillatory motion, which introduces time-dependent behavior into the flow. Rehman et al. [21] employed finite element analysis as a numerical technique to understand the thermal behavior with Casson liquid suspension. Shahzad et al. [22] examined Casson fluid in a bifurcated channel, which is a channel that splits into two or more branches. The channel contains a stenosis, which refers to a constriction in the channel geometry.

Natural convection is the process of heat transfer driven by density differences in a fluid cause by temperature gradients. The phenomena plays an important role in numerous engineering and environmental systems. Understanding the characteristics of buoyancy-induced convection is essential for optimizing heat transfer and energy efficiency in various applications, including geothermal systems, solar collectors, building ventilation, and electronic cooling. Recent research of significance have focus on natural convection. This is evident by contribution registered in the field of buoyancy driven convection. Khan et al. [23] investigated the effects of various factors on natural convection with the used of Casson fluid flow over a plate imbedded with porosity. Alwawi et al. [24] focused on the natural convection of a Casson nanofluid in an enclosure. Consequently, Devi et al. [25] sudied Casson viscoplastic natural convection of fluid flows. Casson fluid under changeable wall circumstances was explored by Anwar et al. [26] taking into account thermal radiative flux and heat injection process with natural convection.

This study will advance the understanding of the thermodynamic efficiency of convective heat transfer systems involving Casson fluids. The findings from this research can guide the design and optimization of various engineering and environmental systems, leading to enhanced energy efficiency and sustainability as well as entropy generation.

2. Mathematical formulation and physical representation

The current study focused on analyzing the behavior of buoyant convective unsteady laminar flow in a square two-dimensional cavity with length (H). The hallow is filled with a type of liquid called Casson liquid through a porous medium. In this study, the left wall of the cavity maintains a constant higher temperature (T_h), while the right wall maintains a constant lower temperature (T_c). The horizontal walls of the enclosure are considered adiabatic. Gravity applied to the y-momentum equation, and thermal radiation is considered in the energy equation. The thermal properties of the liquid remain constant, except for the density term in the buoyancy equation, which follows the Boussinesq approximation. The density of the liquid is defined using the thermal expansion coefficient.

The following are the governing equations for the above problem stated

$$\frac{\partial u}{\partial x}+\frac{\partial v}{\partial y}=0 \tag{1}$$

$$\frac{\partial u}{\partial t}+u\frac{\partial u}{\partial x}+v\frac{\partial u}{\partial y}=-\frac{1}{\rho}\frac{\partial P}{\partial x}+\mu\left(1+\frac{1}{\beta}\right)\nabla^2 u-\mu\left(1+\frac{1}{\beta}\right)\frac{\epsilon^+}{K}u-\frac{F\epsilon^{+^2}}{\sqrt{K}}|V|u \tag{2}$$

$$\frac{\partial v}{\partial t}+u\frac{\partial v}{\partial x}+v\frac{\partial v}{\partial y}=-\frac{1}{\rho}\frac{\partial P}{\partial y}+\mu\left(1+\frac{1}{\beta}\right)\nabla^2 v-\mu\left(1+\frac{1}{\beta}\right)\frac{\epsilon^+}{K}v-\frac{F\epsilon^{+^2}}{\sqrt{K}}|V|v+g\beta(T-T_c) \tag{3}$$

$$\frac{\partial T}{\partial t}+u\frac{\partial T}{\partial x}+v\frac{\partial T}{\partial y}=\frac{k}{\rho c_\rho}\nabla^2 T-\frac{1}{\rho c_\rho}\left[\frac{\partial q_r}{\partial x}+\frac{\partial q_r}{\partial y}\right]+\frac{\mu}{\rho c_\rho}\left(1+\frac{1}{\beta}\right)\frac{v^2}{K}+\frac{\mu}{\rho c_\rho}\left(1+\frac{1}{\beta}\right)\Phi \tag{4}$$

Preprints (www.preprints.org) | NOT PEER-REVIEWED | Posted: 28 July 2023 doi:10.20944/preprints202307.1968.v1

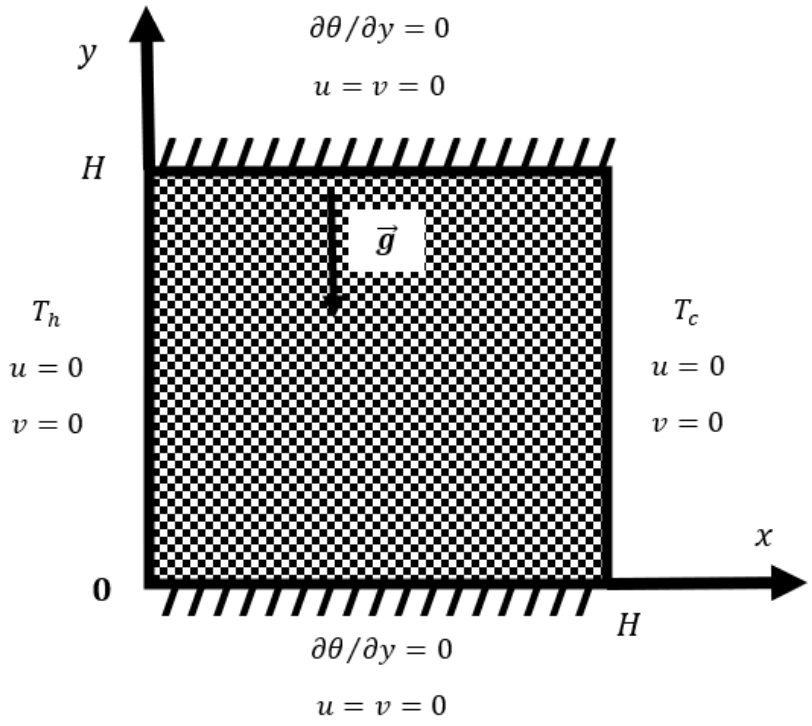

Figure 1. The schematic representation problem statement.

The parameters from Eq.(1)-(4) are specified clearly as (u, v) which is considered dimensional velocity related to components along the (x, y) cartesian coordinate. p is the pressure, T is the local temperature. The density, dynamic viscosity, specific heat, time, casson fluid parameter and thermal conduction are represented as $\rho, \mu, c_\rho, t, \beta$ and k respectively. $K = \dfrac{d^2\epsilon^3}{(150[(1-\epsilon)]^2}$ is considered as permeability of the porous system, where d is the mean particle diameter, the porosity ϵ is classified as the fraction of entire volume in void space. $F = \dfrac{(1.75(1-\epsilon))}{(d\epsilon^3)}$ is the form drag constant, the constant $\dfrac{F}{\sqrt{K}}$ is the Forchheimer number. The norm of the velocity vector $|V| = \sqrt{u^2 + v^2}$, and g represents gravitational acceleration. From Roseland approximate thermal radiation, q_r can be express as $q_{rx} = -\frac{4\sigma^*}{3K'}\dfrac{\partial T^4}{\partial x}$ and $q_{ry} = -\frac{4\sigma^*}{3K'}\dfrac{\partial T^4}{\partial y}$,where K' denotes the absorption coefficient and σ^* the Stefan-Boltzmann constant. Using expansion of Taylor series on T^4 about T_c and dropping high order terms we have

$$T^4 \approx 4TT_c^3 - 3T_c^4,$$

where the viscous dissipation is given as

$$\Phi = 2\left[\left(\frac{\partial \bar{u}}{\partial \bar{x}}\right)^2 + \left(\frac{\partial \bar{v}}{\partial \bar{y}}\right)^2\right] + \left(\frac{\partial \bar{v}}{\partial \bar{x}} + \frac{\partial \bar{u}}{\partial \bar{y}}\right)^2 \tag{5}$$

Eq.(6) represents the dimensionless variables

$$X = \frac{x}{H}, \quad Y = \frac{y}{H}, \quad \tau = \frac{\nu}{H^2}t, \quad \theta = \frac{T - T_c}{T_h - T_c}, \quad u = \frac{\nu}{H}U, \quad v = \frac{\nu}{H}V, \quad P = \frac{H^2}{\rho\nu^2}p \tag{6}$$

we transform Eq.(1) to Eq.(5) by using Eq.(6) to obtained Eq.(7) to Eq.(10)

Preprints (www.preprints.org) | NOT PEER-REVIEWED | Posted: 28 July 2023 doi:10.20944/preprints202307.1968.v1

$$\frac{\partial U}{\partial X}+\frac{\partial V}{\partial Y}=0 \tag{7}$$

$$\frac{\partial U}{\partial \tau}+U\frac{\partial U}{\partial X}+V\frac{\partial U}{\partial Y}=-\frac{\partial P}{\partial X}+\Big(1+\frac{1}{\beta}\Big)\nabla^2 U-\gamma\Big(1+\frac{1}{\beta}\Big)U-\Gamma|V|U \tag{8}$$

$$\frac{\partial V}{\partial \tau}+U\frac{\partial V}{\partial X}+V\frac{\partial V}{\partial Y}=-\frac{\partial P}{\partial Y}+\Big(1+\frac{1}{\beta}\Big)\nabla^2 V-\gamma\Big(1+\frac{1}{\beta}\Big)V-\Gamma|V|V+\frac{Ra}{Pr}\theta \tag{9}$$

$$\frac{\partial \theta}{\partial \tau}+U\frac{\partial \theta}{\partial X}+V\frac{\partial \theta}{\partial Y}=\frac{1}{Pr}\Big(1+\frac{4}{3}Rd\Big)\nabla^2\theta+\frac{Ec}{Da}\Big(1+\frac{1}{\beta}\Big)V^2+Ec\Big(1+\frac{1}{\beta}\Big)\Phi \tag{10}$$

where $\Gamma=\dfrac{l^2F\epsilon^{+^2}}{\sqrt{K}}$ is the Forchheimer number, $\mathrm{Gr}=\dfrac{Ra}{Pr}$ is Grashof number, $Pr=\frac{\nu}{\alpha}$ is Prandtl number, where $\nu=\dfrac{\mu}{\rho}$ is the kinematic viscosity, $\mathrm{Ra}=\dfrac{H^3g\beta(T_h-T_c)}{\alpha\nu}$ is the Rayleigh number, $\gamma=\dfrac{l^2\epsilon^+}{K}$ is the inverse Darcy number. The Darcy number is represented as $\mathrm{Da}=\dfrac{K}{H^2}$, $\mathrm{Rd}=\frac{4\sigma^*T_c^3}{kK'}$ is the radiation parameter, and $\mathrm{Ec}=\dfrac{\nu^2}{c_\rho(T_h-T_c)H^2}$ is the Eckert number.

The Nusselt number signifies the enhancement of convective heat transfer compared to purely conductive heat transfer. A high Nusselt number indicates efficient heat transfer, while a low Nusselt number indicates poor heat transfer.

$$Nu=\Big(1+\frac{4}{3}Rd\Big)\Big(-\frac{\partial\theta}{\partial X}\Big)_{X=0} \tag{11}$$

The average Nusselt number (Nu_{avg}) is used when there are variations in the Nusselt number along the surface. It represents the average convective heat transfer coefficient over the entire surface. It is calculated by integrating the local Nusselt number over the surface and dividing it by the surface area:

$$Nu_{avg}=\int_0^1 NudY \tag{12}$$

2.1. Boundary condition

The dimensionless variables for the conditions stated for initial and boundary are
for $t=0$

$$u=v=\theta=0 \ \text{ for } \ t=0 \qquad\qquad 0\le x,y\le H.$$

for $t>0$

$$x=0,\quad \psi=0,\quad \theta=1,\quad \omega=-\frac{\partial^2\psi}{\partial x^2},\quad 0\le y\le H,$$

$$x=1,\quad \psi=0,\quad \theta=0,\quad \omega=-\frac{\partial^2\psi}{\partial x^2},\quad 0\le y\le H,$$

$$\psi=0,\quad \omega=-\frac{\partial^2\psi}{\partial y^2},\quad \frac{\partial\theta}{\partial y}=0,\quad y=0,l\quad 0\le x\le H. \tag{13}$$

3. Entropy Generation

Entropy generation is a fundamental aspect of thermodynamics, and it plays a crucial role in determining the efficiency and irreversibility of processes. In practical applications, minimizing entropy generation is desirable to improve efficiency and reduce energy losses. When there is a

Preprints (www.preprints.org) | NOT PEER-REVIEWED | Posted: 28 July 2023 doi:10.20944/preprints202307.1968.v1

temperature difference between two bodies, heat transfer occurs from the hotter body to the colder body. This heat transfer process leads to an increase in entropy. The magnitude of entropy generation due to heat transfer depends on the temperature difference, the nature of the heat transfer process (conduction, convection, or radiation), and the efficiency of the process. Friction between surfaces results in energy dissipation and heat generation. This energy dissipation contributes to an increase in entropy. When two surfaces slide or rub against each other, the frictional forces convert mechanical energy into heat. The magnitude of entropy generation due to friction depends on the frictional forces, the relative velocity of the surfaces, and the nature of the frictional contact. The total entropy generation in a system or a process is the sum of entropy generation contributions from all the sources involved. If there are multiple heat transfer processes and frictional interactions occurring simultaneously, the total entropy generation is the sum of entropy generated due to each individual source. Mathematically, Eq.(14) to Eq.(16) shows entropy due to heat, friction and total entropy expressed as:

$$S_{heat} = \left(1+\frac{4}{3}Rd\right)\left[\left(\frac{\partial\theta}{\partial X}\right)^2+\left(\frac{\partial\theta}{\partial Y}\right)^2\right] \tag{14}$$

$$S_{fluid} = \bar{Ec}\left(1+\frac{1}{\beta}\right)\left(2\left[\left(\frac{\partial U}{\partial H}\right)^2+\left(\frac{\partial V}{\partial Y}\right)^2\right]+\left(\frac{\partial U}{\partial Y}+\frac{\partial V}{\partial Y}\right)^2\right)+\frac{\bar{Ec}}{Da}\left(1+\frac{1}{\beta}\right)V^2 \tag{15}$$

$$\begin{aligned} S_{total} = \left(1+\frac{4}{3}Rd\right)\left[\left(\frac{\partial\theta}{\partial X}\right)^2+\left(\frac{\partial\theta}{\partial Y}\right)^2\right]+\bar{Ec}\left(1+\frac{1}{\beta}\right)\left(2\left[\left(\frac{\partial U}{\partial H}\right)^2+\left(\frac{\partial V}{\partial Y}\right)^2\right]\right. \\ \left.+\left(\frac{\partial U}{\partial Y}+\frac{\partial V}{\partial Y}\right)^2\right)+\frac{\bar{Ec}}{Da}\left(1+\frac{1}{\beta}\right)V^2 \end{aligned} \tag{16}$$

4. Code Validation

The computed average Nusselt numbers were compared to available experimental data and established benchmark solutions from Alzahrani et al. [11], Fusegi et al [27], and Ho et al. [28] for for different Rayleigh numbers of ($Ra = 10^3, 10^4, 10^5, 10^6$) in Table 1. The comparison involved a thorough analysis of the deviations, assessing the agreement between the computational and reference work. The results obtained for average Nusselt number were in agreement with existing findings showing minimal error.

Table 1. Average Nusselt number comparison for $Pr = 0.71, Rd = 0, \beta = \infty$.

	Nu_{avg}			
Ra	[11]	[27]	[28]	**Present**
10^3	1.103	1.106	1.118	1.1168
10^4	2.292	2.302	2.246	2.2414
10^5	4.628	4.646	4.522	4.5190
10^6	8.935	9.012	8.825	8.8247

5. Results and Discussion

The results for this investigation is presented in this section. The parameters under study includes Rayleigh number ($10^3 \leq Ra \leq 10^6$), Eckert number ($10^{-6} \leq Ec \leq 10^{-4}$) , Forchheimer number ($0 \leq \Gamma \leq 1$), inverse Darcy ($0 \leq \gamma \leq 1$), radiation ($0 \leq Rd \leq 10$), Prandtl number ($Pr = 0.7, 1.0, 7.0, 10$) and Casson fluid parameters ($0.001 \leq \beta \leq 1$). Figure ($2-10$) shows the effects of dimensionless parameters on streamlines, isotherms, isolines of entropy, velocity, Nusselt number, and total entropy.

5.1. Effects of Rayleigh number

Figure 2 shows for various Rayleigh numbers the streamline, isotherms, and total entropy isoline at fixed parameters $Pr = 10$, $Ec = 10^{-6}$, $Rd = 1$, $\sigma = 0.5$, $\beta = 1$ and $\gamma = 0.25$. The Rayleigh number

Preprints (www.preprints.org) | NOT PEER-REVIEWED | Posted: 28 July 2023 doi:10.20944/preprints202307.1968.v1

affects the flow patterns and the formation of streamlines in a fluid flow. The flow is typically steady and laminar at low Rayleigh numbers $(Ra = 10^3)$, and streamlines follow relatively smooth paths. As the Rayleigh number increases from 10^3 to 10^6 the isotherms are observed to change from smooth and circular single convective core regime to streamlines that exhibit unsteady, more complex and chaotic behavior leading to double convective core regime. Figure 2 presents a near thermal stratification at $Ra = 10^3$. As Rayleigh increases the isotherms tend to exhibit larger temperature differences and more pronounced gradients due to stronger convective heat transfer in natural convection. The Rayleigh number indirectly affects the entropy distribution within the fluid by influencing the temperature distribution. As Ra increase from 10^3 to 10^6 the isolines of entropy are observed to concentrate more on the walls of the cavity as in Figure 2.

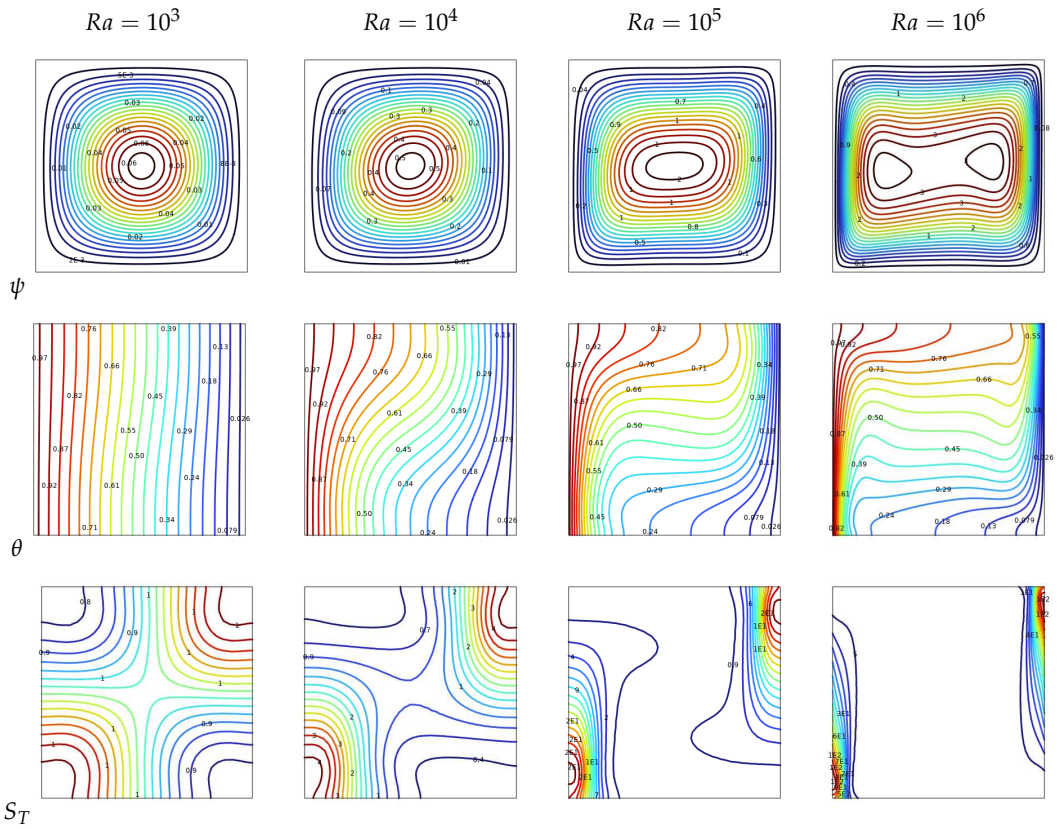

Figure 2. Streamline ψ, isotherms θ, total entropy isolines S_T at, $Pr = 10$,$Ec = 10^{-6}$,$Rd = 1$, $\sigma = 0.5$,$\beta = 1$ and $\gamma = 0.25$ for various Ra.

Figure 3 depicts the velocity, Nusselts number and total entropy for different Rayleigh numbers at fixed parameters $Rd = 2, Ec = 10^{-6}, Pr = 0.7, \gamma = \Gamma = 0.75$. The Rayleigh number also influences the flow velocity distribution in a fluid system. In natural convection, as the Rayleigh number increases, the buoyancy-driven flow becomes more dominant compared to viscous forces. Figure 3a shows that higher Rayleigh numbers tend to induce stronger convective currents, leading to enhanced fluid motion and mixing. For Nusselt number as the Rayleigh number increases, the convective heat transfer becomes more prominent. This leads to larger temperature differences across the fluid and more pronounced temperature gradients (see Figure 3b). Higher Rayleigh numbers often result in increased heat transfer rates and more vigorous thermal mixing. The convective currents and mixing associated with higher Rayleigh numbers contribute to changes in the levels of entropy generation . The effects of entropy are noticed more along the walls of the cavity due to changes in Rayleigh numbers as in Figure 3c.

Preprints (www.preprints.org) | NOT PEER-REVIEWED | Posted: 28 July 2023 doi:10.20944/preprints202307.1968.v1

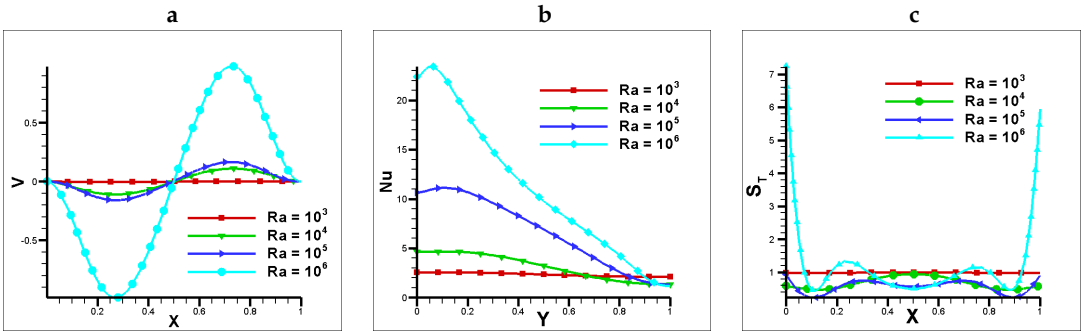

Figure 3. a) Vertical velocity at vertical mid plane, b) Nusselt number at horizontal mid plane c) Total Entropy at vertical mid plane for $Rd = 2, Ec = 10^{-6}, Pr = 0.7, \gamma = \Gamma = 0.75$.

5.2. Effects of Radiation parameter

Figure 4 shows streamline, isotherm, and total entropy isolines at fixed parameters $Pr = 10$, $Ec = 10^{-6}$, $Ra = 10^6$, $\sigma = 0.5$, $\beta = 1$ and $\gamma = 0.25$ for various radiation parameters of $(Rd = 0, 1, 5, 10)$. Streamlines are primarily determined by the fluid's motion and the forces acting upon it, such as pressure gradients and buoyancy. However, radiation can influence the temperature distribution within the fluid, which in turn influences the density distribution and thus the flow patterns. Figure 4 shows that in the absence of radiation $(Rd = 0)$ a double convective core regime is observed and this changes to smooth and single circular core regime as radiation increase to $Rd = 10$. These effects are generally attributed to the fluid movements due to convective heat transmission. The effect on the isotherms as per our case is not showing much significance, this is due to the slow fluid movement cause by the viscoelastic nature of the Casson fluid parameter. Consequently, in Figure 4 the isotherms is notice to deviate as Rd increase which is solely based on the convection heat transfer. As radiation contributes to heat transfer, it can as well impact the local entropy production and distribution. Figure 4 shows that higher radiation levels can lead to increased heat transfer rates and entropy generation within the fluid. The entropy generation analysis are along the walls of the cavity for different radiation parameters

Figure 5 depicts the variation of velocity, Nusselt number and total entropy for different radiation parameters with $Pr = 10$, $Ec = 10^{-6}$, $Ra = 10^6$, $\sigma = 0.5$, $\beta = 1$ and $\gamma = 0.25$. Radiation can contribute to energy exchange within the fluid, resulting in changes in temperature distribution. These temperature variations can then affect fluid density, which in turn can influence fluid motion and velocity. Changes in temperature due to radiation can drive buoyancy forces and induce convective currents, altering the fluid velocity field as presented in Figure 5a. The absorption of radiation by the fluid can increase its temperature, The Nusselt number is affected by the changes in temperature. Figure 5b shows that as radiation increase so does the Nusselt number. The absorption and emission of radiation can lead to local changes in temperature and therefore entropy production within the fluid, which is presented in Figure 5c. Additionally, radiation can influence the entropy exchange between the fluid and its surroundings, contributing to changes in total entropy.

Preprints (www.preprints.org) | NOT PEER-REVIEWED | Posted: 28 July 2023 doi:10.20944/preprints202307.1968.v1

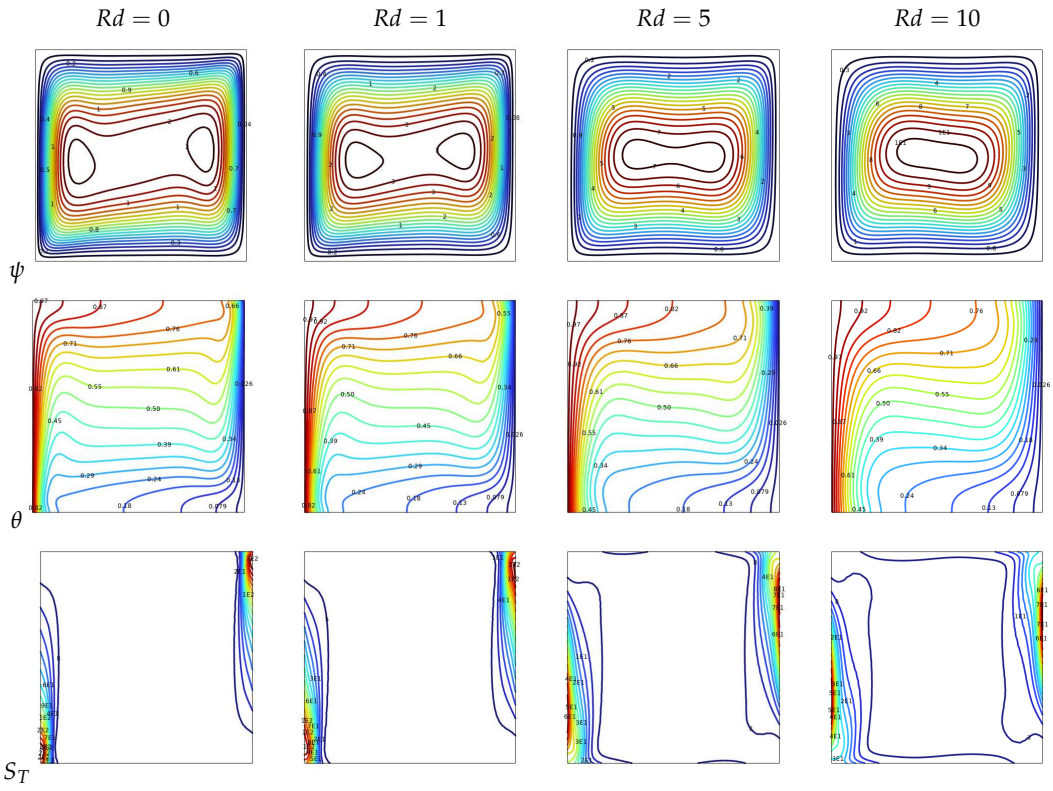

Figure 4. Streamline ψ, isotherms θ, total entropy isolines S_T at, $Pr = 10$, $Ec = 10^{-6}$, $Ra = 10^6$, $\sigma = 0.5$, $\beta = 1$ and $\gamma = 0.25$ for different Rd.

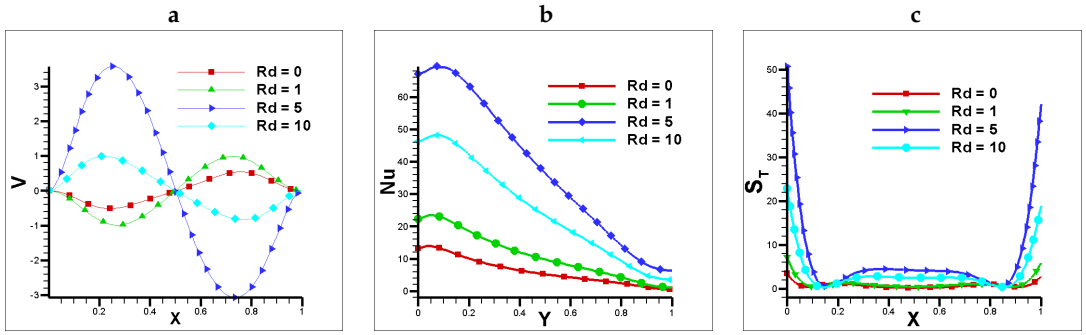

Figure 5. a) Vertical velocity at vertical mid plane, b) Nusselt number at horizontal mid plane c) Total Entropy at vertical mid plane for different Radiation parameters with fixed parameters $Pr = 10$, $Ec = 10^{-6}$, $Ra = 10^6$, $\sigma = 0.5$, $\beta = 1$ and $\gamma = 0.25$.

5.3. Effects of Prandtl number

Figure 6 depict streamline, isotherms and total entropy isolines for various Prandtl numbers at fixed parameters $Ec = 10^{-6}$, $Ra = 10^6$, $Rd = 1$, $\sigma = 0.5$, $\beta = 1$ and $\gamma = 0.25$. The Prandtl number affects the velocity distribution and the boundary layer thickness in a fluid flow. A higher Prandtl number implies a higher thermal diffusivity relative to the kinematic viscosity. As Prandtl changes from $Pr = 0.1$ to $Pr = 10$ the streamlines are more influenced by thermal effects than momentum effects. As a result, with a high Prandtl number, the velocity boundary layer is thinner compared to the thermal boundary layer. For isotherms, the temperature gradients in the fluid are less pronounced, and heat conduction is more dominant compared to convective heat transfer. Consequently, with a high Prandtl number, the isotherms tend to be smoother and less affected by convection (see Figure 6). Similarly for isolines of entropy at higher Prandtl number the heat transfer is relatively more significant than momentum transfer. As a result, the isolines of entropy tend to be more aligned with

Preprints (www.preprints.org) | NOT PEER-REVIEWED | Posted: 28 July 2023 doi:10.20944/preprints202307.1968.v1

the isotherms, reflecting the dominance of thermal effects in the system. Figure 6 shows that isolines cluster around the walls and becomes more pronounce as Prandtl changes from $Pr = 0.1$ to $Pr = 10$.

Figure 7 presents velocity, Nusselt number and total entropy at fixed parameters $Ec = 10^{-6}$, $Ra = 10^6$, $Rd = 1$, $\sigma = 0.5$, $\beta = 1$ and $\gamma = 0.25$. At high Prandtl number $(Pr = 10)$, the velocity boundary layer becomes thinner, and the velocity gradients near the solid boundaries are more pronounced (see Figure 7a). The Prandtl number plays a crucial role in determining the Nusselt number. The Prandtl number appears as an exponent in the Nusselt number correlation, indicating its influence on convective heat transfer. Figure 7b shows that a higher Prandtl number generally leads to a higher Nusselt number, indicating enhanced convective heat transfer. In a fluid flow, entropy is generated due to both heat transfer and fluid friction (viscous dissipation). The Prandtl number influences the ratio between heat transfer and fluid friction effects. A higher Prandtl number implies higher thermal diffusivity relative to the kinematic viscosity. Consequently, with a high Prandtl number, the heat transfer effects dominate over fluid friction effects, resulting in a higher total entropy generation in the system (see Figure 7c).

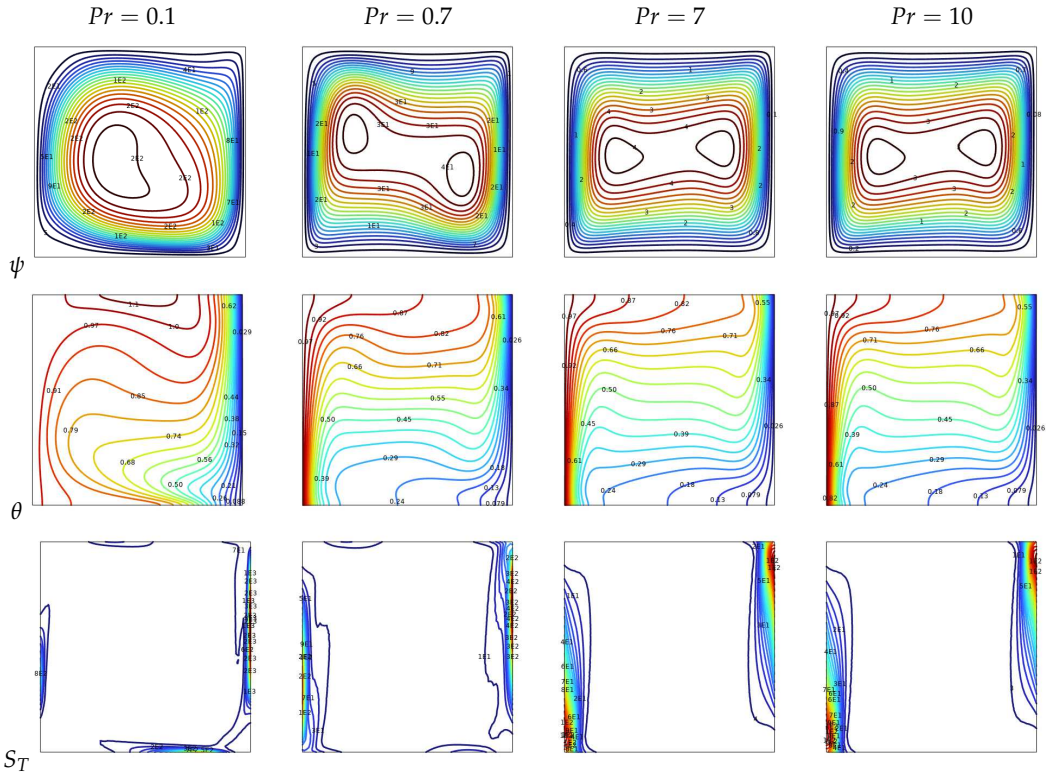

Figure 6. Streamline ψ, isotherms θ, total entropy isolines S_T at, $Ec = 10^{-6}$, $Ra = 10^6$, $Rd = 1$, $\sigma = 0.5$, $\beta = 1$ and $\gamma = 0.25$ for various Pr.

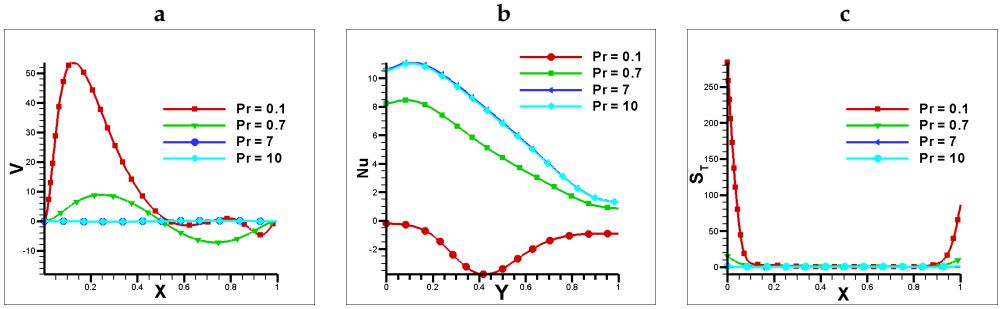

Figure 7. a) Vertical velocity at vertical mid plane, b) Nusselt number at horizontal mid plane c) Total Entropy at vertical mid plane for different Prandtl numbers at $Ec = 10^{-6}$, $Ra = 10^6$, $Rd = 1$, $\sigma = 0.5$, $\beta = 1$ and $\gamma = 0.25$.

Preprints (www.preprints.org) | NOT PEER-REVIEWED | Posted: 28 July 2023 doi:10.20944/preprints202307.1968.v1

5.4. Effects of Casson Fluid Parameter

Figure 8 presents streamline, isotherms, and total entropy isolines for various Casson fluid parameters at $Pr = 10$, $Ec = 10^{-6}$, $Ra = 10^6$, $Rd = 1$, $\sigma = 0.5$ and $\gamma = 0.25$. The Casson fluid parameters, particularly the yield stress, significantly influence the streamlines in the flow. The yield stress represents the minimum stress required to initiate fluid flow. In regions where the applied stress is below the yield stress, the fluid remains stationary, creating a stagnant zone. Figure 8 indicates that as Casson fluid parameter changes from $\beta = 0.001$ to $\beta = 1$ the convective cell cores changes from smooth and circular single cell cores to choatics and double cell cores. The Casson fluid parameters generally have a limited effect on the isotherms, as they primarily describe the rheological behavior of the fluid rather than its thermal characteristics. A near thermal stratification is observed for $\beta = 0.001$ and the isotherms changes significantly for $\beta = 1$ as the temperature gradients increase. This can result in local variations in the temperature distribution and potentially influence the alignment of the isotherms in those regions. The isolines of entropy in a Casson fluid flow tend to exhibit more pronounced gradients and deviations due to the additional energy dissipation and flow complexity associated with the yield stress behavior as the casson fluid parameter increase (see Figure 8).

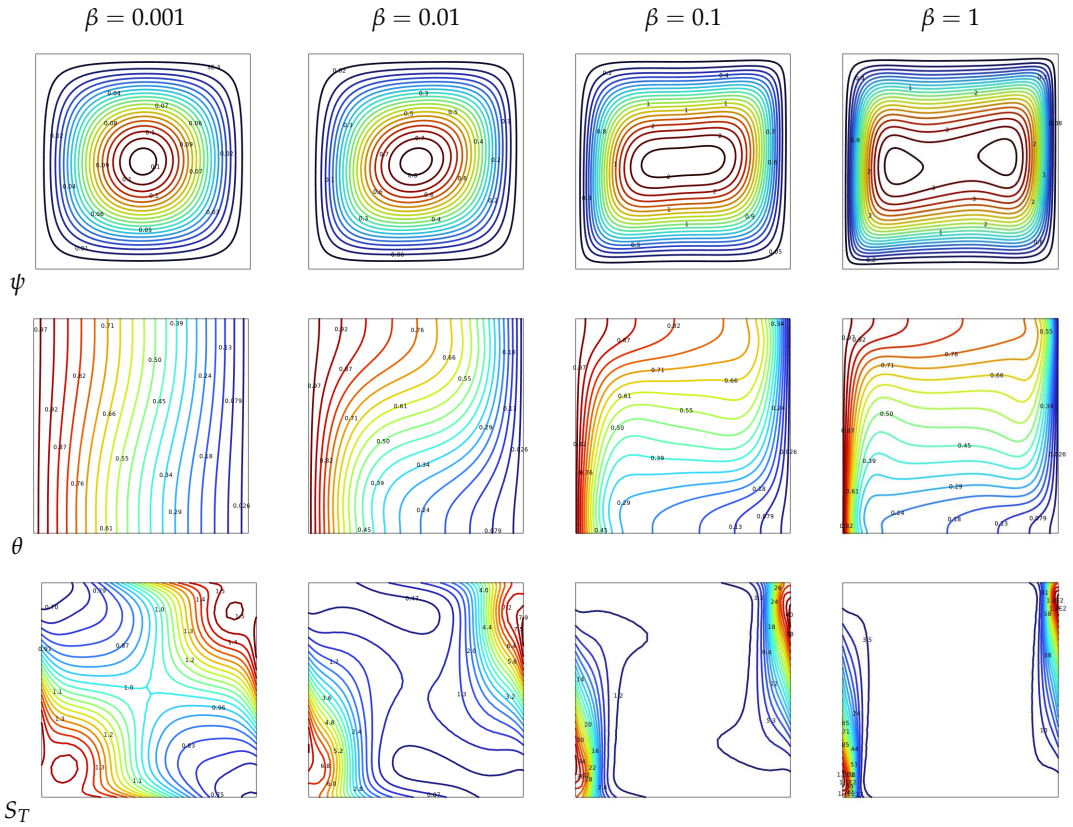

Figure 8. Streamline ψ, isotherms θ, total entropy isolines S_T at, $Pr = 10$,$Ec = 10^{-6}$, $Ra = 10^6$, $Rd = 1$, $\sigma = 0.5$ and $\gamma = 0.25$ for various β.

Figure 9 depicts the velocity, Nusselt number and total entropy for various Casson fluid parameters with $Pr = 10$, $Ec = 10^{-6}$, $Ra = 10^6$, $Rd = 1$, $\sigma = 0.5$ and $\gamma = 0.25$. Higher values of the Casson fluid parameter indicates a higher yield stress and a more significant resistance to flow. As a result, the velocity profile becomes more flattened near the boundaries, and the fluid tends to move with a higher velocity in the central region of the flow. The yield stress acts as a barrier, requiring a certain amount of shear stress to initiate the flow. Therefore, a higher Casson fluid parameter leads to reduced velocities near the boundaries and increased velocities in the core region of the flow (see Figure 9a). Higher values of the Casson fluid parameter leads to lower Nusselt numbers, indicating a reduced

Preprints (www.preprints.org) | NOT PEER-REVIEWED | Posted: 28 July 2023 doi:10.20944/preprints202307.1968.v1

convective heat transfer as observed in Figure 9b. The presence of a yield stress and non-Newtonian behavior leads to additional energy dissipation and increased entropy generation. The Casson fluid parameter influences the flow behavior, velocity gradients, and shear stresses in the fluid. Figure 9c shows that higher values of the Casson fluid parameter generally result in increased total entropy generation in the flow due to the greater resistance and energy dissipation associated with the yield stress behavior.

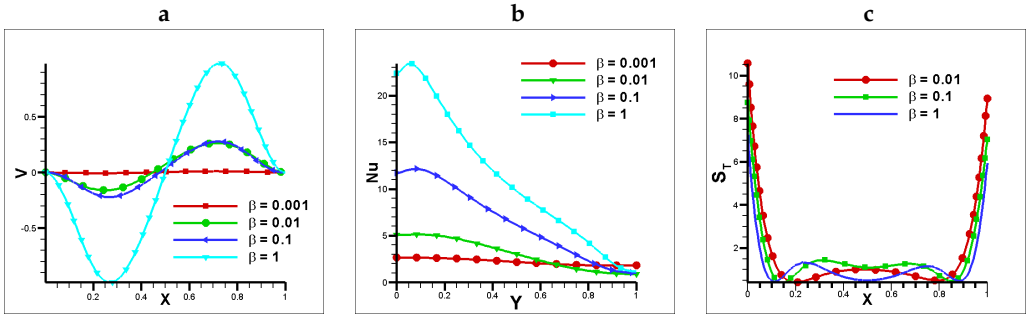

Figure 9. a) Vertical velocity at vertical mid plane, b) Nusselt number at horizontal mid plane c) Total Entropy at vertical mid plane for for different Casson fluid parameters at $Pr = 10$, $Ec = 10^{-6}$, $Ra = 10^6$,$Rd = 1$, $\sigma = 0.5$ and $\gamma = 0.25$.

5.5. Effects of Time

For varying Rayleigh values, the velocity, average Nusselt number, and total entropy are presented against time in Figure 10. As the Rayleigh number in the flow pattern increase over time, the velocity diminishes and attained a uniform flow phenomena. This is because in convective heat transfer, velocity fluctuations promote the exchange of thermal energy between the fluid and solid surfaces, leading to enhanced heat transfer rates. In buoyancy-driven flows, the Rayleigh number influences the evolution of the average Nusselt number and total entropy over time. When the flow begins or the temperature distribution changes the Nu_avg and S_T is observed to follow a uniform flow pattern as time evolves (see Figure 10b,c).

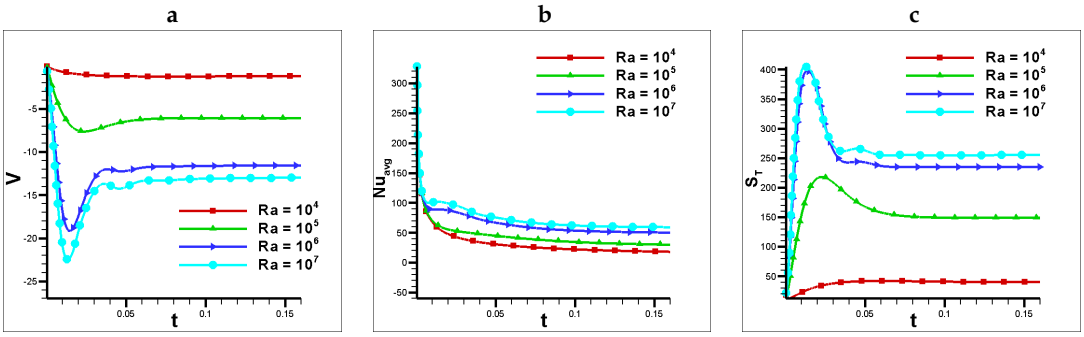

Figure 10. a) Velocity with time , b) Average Nusselt number with time c) Total Entropy with time at $Pr = 10$, $Ec = 10^{-6}$, $Rd = 1$, $\beta = 1$, $\sigma = 0.5$ and $\gamma = 0.25$.

6. Conclusion

In conclusion, this study has successfully investigated the entropy generation characteristics during natural convection in a porous medium with Casson fluid, utilizing the Finite Element Method which provides accurate modeling and simulation capabilities, enabling a detailed analysis of the complex fluid flow and heat transfer phenomena. The analysis has provided valuable insights into the complex interplay between fluid flow, heat transfer, and entropy generation in such systems. Through numerical simulations and analysis, the study revealed the significant influence of the Casson fluid parameter, Darcy number, Prandtl number, and Rayleigh number on the entropy generation rate.

The Casson fluid parameter, which consider the non-Newtonian behavior of the fluid, was observed to have an important impact on the flow and heat transfer characteristics. The Darcy number and Rayleigh number controlled the intensity of natural convection, while the Prandtl number determined the relative significance of the heat transfer as compared to viscous effects.

The findings of this study contribute to the advancement of fundamental knowledge in heat transfer, fluid dynamics, and entropy generation. The use of a porous medium will enhanced and ensure the realism of the model, accounting for its significant influence on the system behavior.

References

1. Saboj, Jiaul Haque, Nag, Preetom, Saha, Goutam and Saha, Suvash C. "Entropy Production Analysis in an Octagonal Cavity with an Inner Cold Cylinder: A Thermodynamic Aspect." Energies 16(14) (2023): 5487; https://doi.org/10.3390/en16145487.
2. Saha, Goutam, Al-Waaly, Ahmed A.Y., Paul, Manosh C. and Saha, Suvash C. "Heat Transfer in Cavities: Configurative Systematic Review" Energies 16(5) (2023): 2338; https://doi.org/10.3390/en16052338
3. Pop, Ioan, and Mikhail Sheremet. "Free convection in a square cavity filled with a Casson fluid under the effects of thermal radiation and viscous dissipation." International Journal of Numerical Methods for Heat & Fluid Flow 27.10 (2017): 2318-2332.
4. Hamid, M., et al. "Heat transfer and flow analysis of Casson fluid enclosed in a partially heated trapezoidal cavity." International Communications in Heat and Mass Transfer 108 (2019): 104284.
5. Aneja, Madhu, Avinash Chandra, and Sapna Sharma. "Natural convection in a partially heated porous cavity to Casson fluid." International Communications in Heat and Mass Transfer 114 (2020): 104555.
6. Aghighi, M. S., A. Ammar, and H. Masoumi. "Double-diffusive natural convection of Casson fluids in an enclosure." International Journal of Mechanical Sciences 236 (2022): 107754.
7. Shah, Imtiaz Ali, et al. "Convective Heat and Mass Transport in Casson Fluid Flow in Curved Corrugated Cavity with Inclined Magnetic Field." Micromachines 13.10 (2022): 1624.
8. Gireesha, B. J., et al. "Entropy generation and heat transport analysis of Casson fluid flow with viscous and Joule heating in an inclined porous microchannel." Proceedings of the Institution of Mechanical Engineers, Part E: Journal of Process Mechanical Engineering 233.5 (2019): 1173-1184.
9. Kotha, Gangadhar, and Ali J. Chamkha. "Entropy generation on convectively heated surface of casson fluid with viscous dissipation." Physica Scripta 95.11 (2020): 115203.
10. Sohail, Muhammad, et al. "Entropy generation in MHD Casson fluid flow with variable heat conductance and thermal conductivity over non-linear bi-directional stretching surface." Scientific Reports 10.1 (2020): 12530.
11. Alzahrani, A. K., Sivanandam Sivasankaran, and M. Bhuvaneswari. "Numerical simulation on convection and thermal radiation of Casson fluid in an enclosure with entropy generation." Entropy 22.2 (2020): 229.
12. Hussain, Shafqat, Shahin Shoeibi, and Taher Armaghani. "Impact of magnetic field and entropy generation of Casson fluid on double diffusive natural convection in staggered cavity." International Communications in Heat and Mass Transfer 127 (2021): 105520.
13. Seth, Gauri Shanker, and Prashanta Kumar Mandal. "Hydromagnetic rotating flow of Casson fluid in Darcy-Forchheimer porous medium." MATEC Web of Conferences. Vol. 192. EDP Sciences, 2018.
14. Qawasmeh, Bashar R., Mohammad Alrbai, and Sameer Al-Dahidi. "Forced convection heat transfer of Casson fluid in non-Darcy porous media." Advances in Mechanical Engineering 11.1 (2019): 1687814018819906.
15. Farooq, Umer, et al. "Modeling and non-similar analysis for Darcy-Forchheimer-Brinkman model of Casson fluid in a porous media." International Communications in Heat and Mass Transfer 119 (2020): 104955.
16. Zhang, Xianqin, et al. "Heat transport phenomena for the Darcy–Forchheimer flow of Casson fluid over stretching sheets with electro-osmosis forces and Newtonian heating." Mathematics 9.19 (2021): 2525.
17. Li, Shuguang, et al. "Effects of activation energy and chemical reaction on unsteady MHD dissipative Darcy–Forchheimer squeezed flow of Casson fluid over horizontal channel." Scientific Reports 13.1 (2023): 2666.

18. Raju, R. Srinivasa, B. Mahesh Reddy, and G. Jithender Reddy. "Finite element solutions of free convective Casson fluid flow past a vertically inclined plate submitted in magnetic field in presence of heat and mass transfer." International Journal for Computational Methods in Engineering Science and Mechanics 18.4-5 (2017): 250-265.
19. Reddy, G. Jithender, R. Srinivasa Raju, and J. Anand Rao. "Influence of viscous dissipation on unsteady MHD natural convective flow of Casson fluid over an oscillating vertical plate via FEM." Ain Shams Engineering Journal 9.4 (2018): 1907-1915.
20. Goud, B. Shankar, P. Pramod Kumar, and Bala Siddulu Malga. "Effect of heat source on an unsteady MHD free convection flow of Casson fluid past a vertical oscillating plate in porous medium using finite element analysis." Partial Differential Equations in Applied Mathematics 2 (2020): 100015.
21. Rehman, Khalil Ur, et al. "On thermally corrugated porous enclosure (TCPE) equipped with casson liquid suspension: Finite element thermal analysis." Case Studies in Thermal Engineering 25 (2021): 100873.
22. Shahzad, Hasan, et al. "Fluid structure interaction study of non-Newtonian Casson fluid in a bifurcated channel having stenosis with elastic walls." Scientific Reports 12.1 (2022): 12219.
23. Khan, Dolat, et al. "Effects of relative magnetic field, chemical reaction, heat generation and Newtonian heating on convection flow of Casson fluid over a moving vertical plate embedded in a porous medium." Scientific reports 9.1 (2019): 400.
24. Alwawi, Firas A., et al. "MHD natural convection of Sodium Alginate Casson nanofluid over a solid sphere." Results in physics 16 (2020): 102818.
25. Devi, T. Sarala, et al. "Simulation of unsteady natural convection flow of a Casson viscoplastic fluid in a square enclosure utilizing a MAC algorithm." Heat Transfer 49.4 (2020): 1769-1787.
26. Anwar, Talha, Poom Kumam, and Wiboonsak Watthayu. "Unsteady MHD natural convection flow of Casson fluid incorporating thermal radiative flux and heat injection/suction mechanism under variable wall conditions." Scientific Reports 11.1 (2021): 4275.
27. Fusegi, T., et al. "A numerical study of three-dimensional natural convection in a differentially heated cubical enclosure." International Journal of Heat and Mass Transfer 34.6 (1991): 1543-1557.
28. Ho, Ching-Jenq, M. W. Chen, and Z. W. Li. "Numerical simulation of natural convection of nanofluid in a square enclosure: effects due to uncertainties of viscosity and thermal conductivity." International Journal of Heat and Mass Transfer 51.17-18 (2008): 4506-4516.